INSTITUTE OF PHYSICS PUBLISHING JOURNAL OF PHYSICS B: ATOMIC, MOLECULAR AND OPTICAL PHYSICS

J. Phys. B: At. Mol. Opt. Phys. **35** (2002) 1455–1465 PII: S0953-4075(02)28977-4

Stopping power and polarization induced in a plasma by a fast charged particle in circular motion

Isidro Villó-Pérez[1], **Néstor R Arista**[2] **and Rafael Garcia-Molina**[3]

[1] Departamento de Electrónica, Tecnología de las Computadoras y Proyectos, Universidad Politécnica de Cartagena, E-30202, Cartagena, Spain
[2] División Colisiones Atómicas, Centro Atómico Bariloche and Instituto Balseiro, Comisión Nacional de Energía Atómica, RA-8400 Bariloche, Argentina
[3] Departamento de Física, Universidad de Murcia, Apartado 4021, E-30080 Murcia, Spain

Received 17 September 2001, in final form 22 January 2002
Published 13 March 2002
Online at stacks.iop.org/JPhysB/35/1455

Abstract

We describe the perturbation induced in a plasma by a charged particle in circular motion, analysing in detail the evolution of the induced charge, the electrostatic potential and the energy loss of the particle. We describe the initial transitory behaviour and the different ways in which convergence to final stationary solutions may be obtained depending on the basic parameters of the problem. The results for the stopping power show a resonant behaviour which may give place to large stopping enhancement values as compared with the case of particles in straight-line motion with the same linear velocity. The results also explain a resonant effect recently obtained for particles in circular motion in magnetized plasmas.

1. Introduction

The perturbation produced by swift charged particles in a plasma has been studied extensively over the years using various theoretical approaches [1–4], and some of these developments have also been widely used in the case of swift ionized particles in solids [5–10]. It is well known from these studies that the perturbation induced in the medium as a result of the dynamical screening by the plasma electrons shows an important oscillatory density wave trailing behind the projectile and moving collectively with the same projectile velocity. This wake field has important effects on the excitations produced in the medium as well as on the dynamics of other moving particles [5–12]. The shape of this wake has been described in previous references but only for the case of ions moving along straight trajectories.

On the other hand, recent studies of the interaction of charged particles with magnetized plasmas [13, 14] have described the changes in the energy loss of the particles by the effect of strong magnetic fields. These studies have been made using both classical [13] and quantum mechanical [14] formulations, following the lines of the dielectric formalism. The results are of interest for studies of energy dissipation of particles in magnetized plasmas and cover a very

wide range of systems, including laboratory plasmas for inertial confinement fusion research, for instance, as well as several other systems of astrophysical interest, such as white dwarfs and neutron stars where very high magnetic fields are produced. For a general description of the different cases of interest we refer the reader to the references quoted before. Here we shall concentrate on the study of one of the most interesting results emerging from these studies, which is the appearance of a pronounced resonance effect in the energy loss of particles moving along circular trajectories, with velocities perpendicular to the magnetic field lines [13, 14]. These resonances may be tuned up by changing the value of the magnetic field.

The purpose of this work is to analyse this resonance phenomenon. Here we analyse in detail the characteristics of the perturbation induced by a charged particle in circular motion within the plasma. In the present description we shall use a different approach, which, although being fully compatible with the previous ones [13, 14], permits us to understand in a detailed way the origin of the resonance effect, as well as the approach to the equilibrium situation described in the previous papers. In particular, we shall consider here the shape of the induced potential and the build-up of the screening charge around the test particle, and shall finally describe the modifications in the energy loss of the particle as compared with the better known case of particles in straight trajectories. Due to the periodicity of the circular motion, we shall show the occurrence of resonance (or antiresonance) conditions, which may have a large effect on the energy loss rate. The results of this study will be compared with recent calculations of the energy loss rate of particles in magnetized plasmas [13, 14]. As will be shown, the present study provides a microscopic explanation of the resonance effects previously obtained in the case of particles moving perpendicularly to an external magnetic field within the plasma.

The paper is organized as follows: in the next section we describe the calculation of the induced charge and potential, and derive the stopping power. In section 3 we show the results of our calculations, and finally, in section 4, we discuss the results and the relationship with previous studies for particles in magnetized plasmas.

2. Formulation

2.1. Induced charge and potential

We consider a point particle with charge Ze moving with angular velocity Ω in a circular orbit of radius a with centre in the origin of a Cartesian coordinate frame. In order to describe the transitory response of the medium, we assume that at $t = 0$ the particle begins its motion with speed $v = \Omega a$ at the point $(x = a, y = 0)$. In this case the charge density ρ_f associated with the particle, in cylindrical coordinates (ρ, φ, z), is given by

$$\rho_f(\boldsymbol{r}, t) = Zeu(t)\delta(z)\frac{\delta(\rho - a)}{\rho}\delta[\varphi - (\Omega t - 2\pi m(t))], \tag{1}$$

where $u(t)$ is the unit step function: $u(t) = 0$ for $t < 0$, $u(t) = 1$ for $t \geqslant 0$ and $m(t)$ is a multistep function, given by

$$m(t) = \begin{cases} 0, & \text{if } t \in [0, T_0) \\ 1, & \text{if } t \in [T_0, 2T_0) \\ 2, & \text{if } t \in [2T_0, 3T_0), \ldots, \end{cases} \tag{2}$$

with $T_0 = 2\pi/\Omega$ being the period of the circular motion.

In order to describe the response of the medium, we employ the macroscopic dielectric function in the high-frequency limit with a plasma frequency ω_p and damping constant γ, which describes the plasma resonance behaviour for frequencies $\omega \sim \omega_p$,

$$\varepsilon(\omega) = 1 - \frac{\omega_p^2}{\omega(\omega + \mathrm{i}\gamma)}. \tag{3}$$

This form of the plasma resonance is particularly useful to study the response of the system in the case of fast particles moving with velocities perpendicular to the magnetic field lines [13] as in the present case.

From a Fourier analysis of the corresponding functions, we obtain the relation between the induced charge density (ρ_{ind}) and the free charge density associated with the particle (ρ_f) in the frequency domain as

$$\rho_{ind}(\boldsymbol{r}, \omega) = \xi(\omega)\rho_f(\boldsymbol{r}, \omega), \tag{4}$$

where

$$\xi(\omega) \equiv \frac{1}{\varepsilon(\omega)} - 1. \tag{5}$$

Taking the inverse Fourier transform of equation (4), we obtain the following relation in the time domain:

$$\rho_{ind}(\boldsymbol{r}, t) = \int_{-\infty}^{\infty} \xi(t - t')\rho_f(\boldsymbol{r}, t')\,\mathrm{d}t', \tag{6}$$

where $\xi(t)$ is the time-inverse Fourier transform of equation (5).

Inserting equation (3) in (5), the following temporal response function is obtained after integration:

$$\xi(t) = -\frac{\omega_p^2}{\omega_p'} \sin(\omega_p' t)\mathrm{e}^{-(\gamma/2)t} u(t), \tag{7}$$

where $\omega_p' \equiv \sqrt{\omega_p^2 - \gamma^2/4}$.

Substituting equations (1) and (7) in (6), we finally obtain the polarization charge density induced in the medium

$$\rho_{ind}(\boldsymbol{r}, t) = -\frac{Ze\omega_p^2}{\Omega\omega_p'} \frac{\delta(\rho - a)\delta(z)}{\rho} \sum_n \sin(\omega_p' \tau_n)\mathrm{e}^{-\frac{\gamma}{2}\tau_n} u(\tau_n), \tag{8}$$

with

$$\tau_n \equiv \frac{\Omega t - 2\pi n - \varphi}{\Omega}, \qquad n = 0, 1, 2, \ldots. \tag{9}$$

This distribution corresponds to a line of charge extending along the circular orbit. Notice that the step function $u(\tau_n)$ introduces a cut-off (or a maximum value of n) such that the number of terms in the sum increases with time according to the value of the parameter τ_n.

From the above equation it is straightforward to derive the induced electric potential

$$\phi_{ind}(\boldsymbol{r}, t) = \int_0^{2\pi} \frac{\lambda_{ind}(\varphi', t)a\,\mathrm{d}\varphi'}{\sqrt{\rho_0^2 + \rho^2 + a^2 - 2\rho a\cos(\varphi - \varphi') + z^2}}, \tag{10}$$

where

$$\lambda_{ind}(\varphi, t) = -A \sum_n \sin(\omega_p' \tau_n)\mathrm{e}^{-(\gamma/2)\tau_n} u(\tau_n) \tag{11}$$

is the induced linear charge density, with

$$A = \frac{Ze\omega_p^2}{v\omega_p'}. \tag{12}$$

In equation (10) $\rho_0 = \hbar/2mv$ is a quantum cut-off value which takes into account the behaviour of the response function in the short-wavelength limit as described in previous papers [7,8,12]; m is the electron mass.

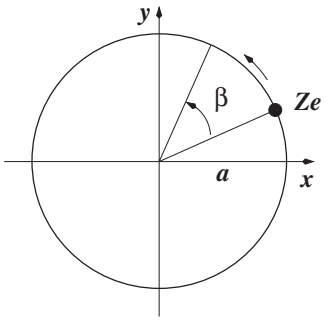

Figure 1. Illustration of the parameters used in this description: charge Ze moving along a circle of radius a within a plasma. The values of the induced potential and charge density will be analysed in terms of the relative angular coordinate β ($0 < \beta < 2\pi$).

Notice that in equation (11) the spatial periodicity (in the angular dependence) of the function $\sin(\omega'_p \tau_n)$ is characterized in terms of the parameter

$$\kappa \equiv \frac{\omega'_p}{\Omega} = \frac{a\omega'_p}{v}. \tag{13}$$

From the analysis of equation (11) we observe the following.

(a) If $\gamma = 0$ and $\kappa = (2\ell + 1)/2$ ($\ell = 0, 1, 2 \ldots$), then the sine functions in the sum cancel each other out pairwise, so the charge induced in a given period is cancelled by the charge induced in the following period.

(b) If $\gamma = 0$ and $\kappa = \ell + 1$, then the charge induced in each period contributes with an identical additional term, leading to a growing accumulation of charge.

In the first case, the particle sees an oscillatory induced charge which is turned on and off with a time period T_0. In the second, the particle sees a permanently growing induced charge. In both cases one obtains nonstationary solutions.

We shall show now that when $\gamma > 0$ the induced charge, and therefore also the potential, reaches in all cases a final stationary state, as seen from a frame of reference that rotates with the particle. For this purpose we take a point of observation whose angular coordinate φ changes with time according to the law

$$\varphi_\beta(t) = \Omega t + \beta - 2\pi m'(t) \tag{14}$$

where β is an angular coordinate that varies in the restricted interval $[0, 2\pi)$, and $m'(t)$ is a multistep-like function with the following behaviour:

$$m'(t) = \begin{cases} 0, & \text{if } t \in [0, T_0 - \beta/\Omega) \\ 1, & \text{if } t \in [T_0 - \beta/\Omega, 2T_0 - \beta/\Omega) \\ 2, & \text{if } t \in [2T_0 - \beta/\Omega, 3T_0 - \beta/\Omega), \ldots . \end{cases} \tag{15}$$

In this way, the variable β denotes a *relative* angular coordinate corresponding to an observation point which stays stationary with respect to the moving particle, and is situated (on the orbit) at an angle β measured from the instantaneous position of the particle, in the anti-clockwise direction, as illustrated in figure 1.

Using equation (14) in (9) we observe that equation (11) may be expressed as a function of (β, t), taking

$$\tau_n = \frac{2\pi(m'(t) - n) - \beta}{\Omega} \tag{16}$$

which yields the time evolution of the induced charge at the observation point with $\varphi = \varphi_\beta(t)$.

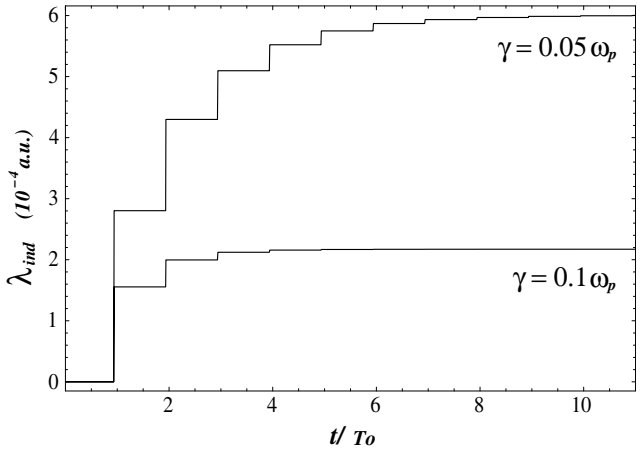

Figure 2. Evolution of the induced linear charge density λ_{ind}, equation (11), for a point located on the orbit of the particle and at a relative angular position $\beta = \pi/8$ ahead of the particle (moving with the same angular frequency as the particle), as a function of time t, for $v = 2.7$ au, $a = 4v/\omega_p'$, $\omega_p = 1.364 \times 10^{-3}$ au and for $\gamma = 0.05\omega_p$ and $0.1\omega_p$. The steps in the values of λ_{ind} occur when a new orbital period is completed. The value of the damping constant γ has an important influence on the convergence of the series and on the final asymptotic value.

2.2. Stopping power

From equation (10) we can obtain the induced electric field $\boldsymbol{E}_{ind}(\boldsymbol{r}, t) = -\boldsymbol{\nabla}\phi_{ind}(\boldsymbol{r}, t)$ and then calculate the stopping force, or energy loss per unit distance, $F = \mathrm{d}E/\mathrm{d}l = Ze\boldsymbol{E}_{ind}(\boldsymbol{r}, t)\cdot\boldsymbol{\varphi}|_{r=r_0(t)}$ (where $\mathrm{d}l$ denotes a differential pathlength along the circular trajectory). Hence, we define the instantaneous stopping power as

$$S(t) \equiv -\left.\frac{\mathrm{d}E}{\mathrm{d}l}\right|_t = \frac{Ze}{a}\left.\frac{\partial\phi_{ind}(\boldsymbol{r}, t)}{\partial\varphi}\right|_{r=r_0(t)} \tag{17}$$

where the derivative is calculated at the instantaneous position of the particle, $\boldsymbol{r}_0(t) = (\rho = a,\ \varphi = \Omega t - 2\pi m(t),\ z = 0)$. We obtain in this way

$$S(t) = -Zea^2\int_0^{2\pi}\frac{\lambda_{ind}(\varphi', t)\sin\left[\Omega t - 2\pi m(t) - \varphi'\right]\mathrm{d}\varphi'}{\{\rho_0^2 + 2a^2[1 - \cos\left(\Omega t - 2\pi m(t) - \varphi'\right)]\}^{\frac{3}{2}}}. \tag{18}$$

3. Results

In figures 2–6 we show the results of calculations of induced charge and electric potential for various situations. The present calculations correspond to an ion of unit charge ($Z = 1$) in a plasma with a fixed plasma frequency ω_p for various values of the damping constant γ, particle speed v and circular radius a. For comparative purposes we use here the same values as in [13] (electron density $n = 10^{18}$ cm^3 and plasma frequency $\omega_p = \sqrt{4\pi ne^2/m} = 5.64 \times 10^{13}$ s^{-1}). In the following the values of the quantities will be given in atomic units (in particular, $\omega_p = 1.364 \times 10^{-3}$ au). Note that all the values used here may be re-scaled to represent other physical situations.

In figure 2 we show the evolution of the induced linear charge density λ_{ind} for a point on the circular orbit at a relative angular position $\beta = \pi/8$ ahead of the particle, as a function of time t, for a velocity $v = 2.7$ au and for $\gamma = 0.05\omega_p$ and $0.1\omega_p$. We observe that the value of

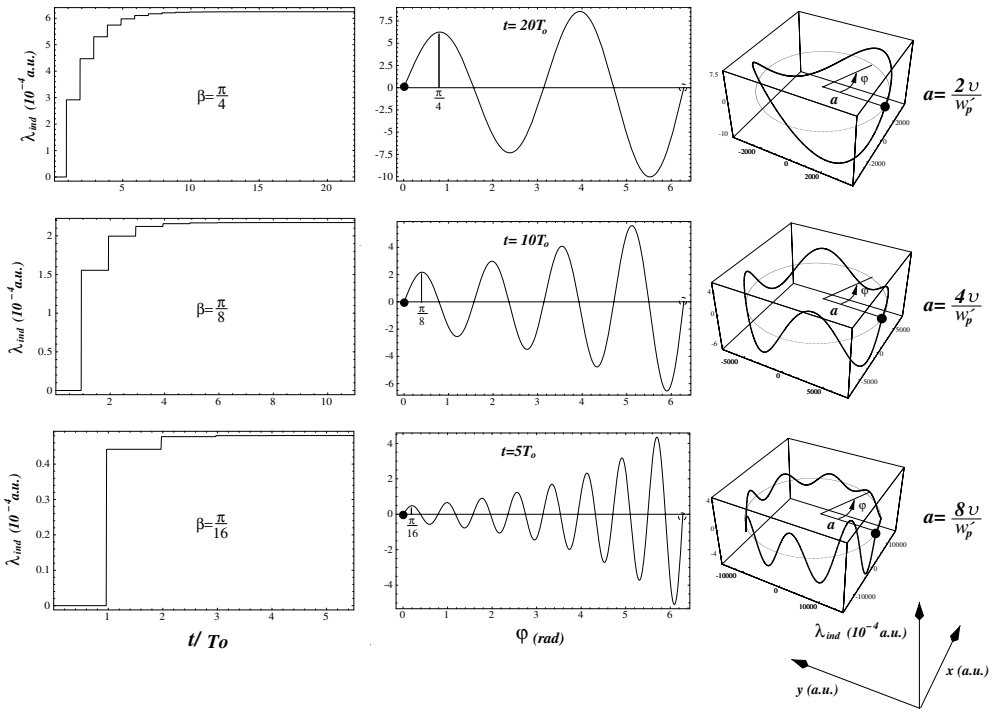

Figure 3. Calculations of the induced linear charge density for a fixed velocity $v = 2.7$ au and for three values of the orbit radius ($a = 2v/\omega'_p$, $4v/\omega'_p$ and $8v/\omega'_p$); $\omega_p = 1.364 \times 10^{-3}$ au, and $\gamma = 0.1\omega_p$. The left-hand panels show the values of the induced linear density at the reference positions $\beta = \pi/4$, $\pi/8$ and $\pi/16$, as a function of time. The central panels show the whole variation of the induced linear density along the trajectory circle ($0 < \varphi < 2\pi$) at fixed times, $t/T_0 = 20, 10$ and 5, respectively. The values indicated by vertical lines correspond to the saturation values (for the particular positions $\beta = \pi/4$, $\pi/8$ and $\pi/16$) shown in the left-hand panels. The panels on the right illustrate the whole behaviour of λ_{ind}. These wake structures rotate together with the particle once the final equilibrium state is reached (i.e., they are stationary with respect to the particle).

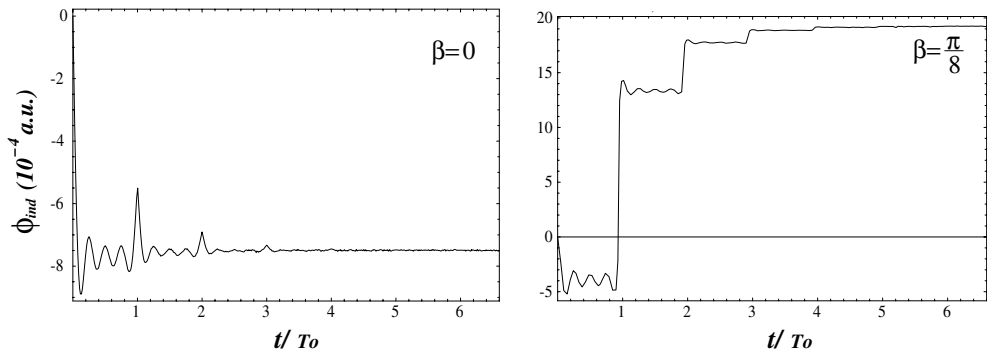

Figure 4. Values of the induced potential ϕ_{ind} on reference points along the trajectory with $\beta = 0$ and $\pi/8$. Calculations correspond to $v = 2.7$ au, $\omega_p = 1.364 \times 10^{-3}$ au, $\gamma = 0.1\omega_p$ and $a = 4v/\omega'_p$.

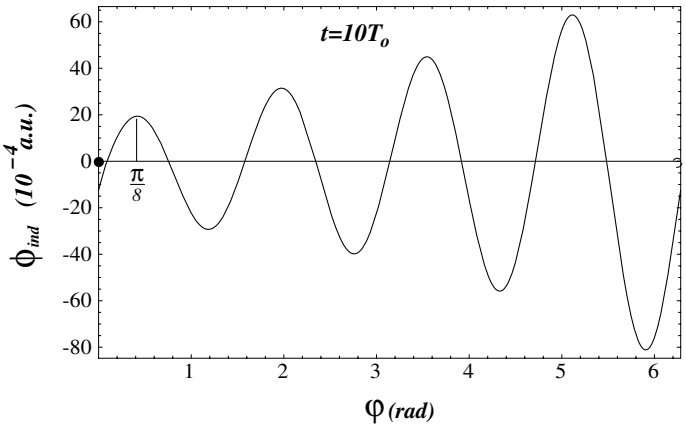

Figure 5. Instantaneous values of the induced potential $\phi_{ind}(\rho = a, \varphi, z = 0)$ as a function of coordinate φ at a time $t = 10T_0$, and for $v = 2.7$ au, $\omega_p = 1.364 \times 10^{-3}$ au, $\gamma = 0.1\omega_p$ and $a = 4v/\omega_p'$. The solid point at the origin indicates the instantaneous position of the charge.

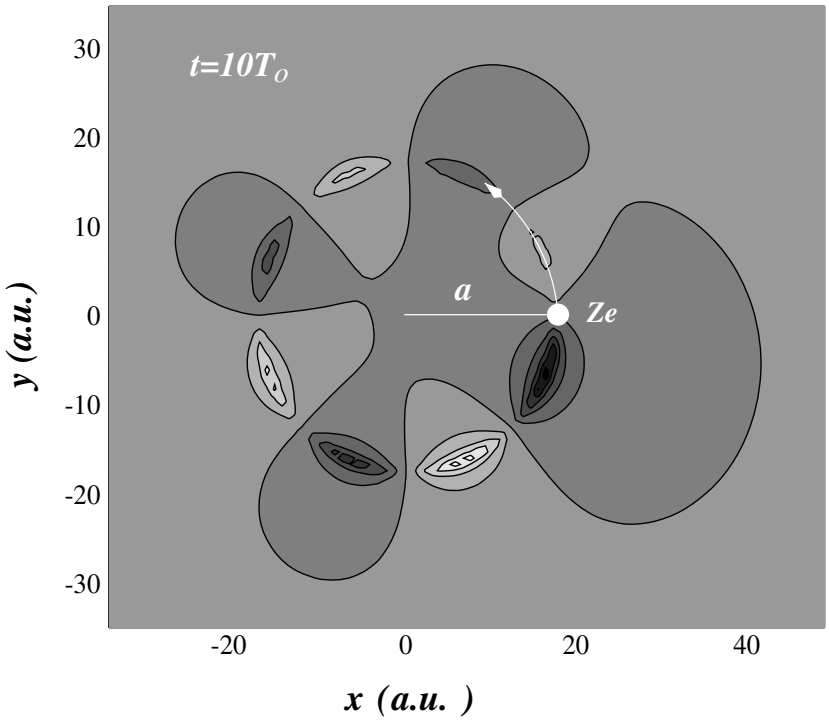

Figure 6. Instantaneous view of the wake potential on the plane of the motion ($z = 0$), namely $\phi_{ind}(\rho, \varphi, z = 0)$, for $v = 2.7$ au, $\omega_p = 1.364 \times 10^{-3}$ au, $\gamma = 0.1\omega_p$, $a = 4v/\omega_p'$ and $t = 10T_0$.

λ_{ind} increases by steps every time a new period is completed. The case $\gamma = 0.05\omega_p$ illustrates how in the case of small damping the value of λ_{ind} shows a large increasing behaviour (which diverges when $\gamma = 0$). In fact, the finite value of γ provides the attenuation factor which allows convergence of the series. Thus, for $\gamma = 0.1\omega_p$ a smaller saturation value of λ_{ind} is obtained (and a faster convergence), as also seen in the figure.

In figure 3 we show calculations for a fixed speed $v = 2.7$ au, and for three values of the orbit radius: $a = 2v/\omega_p'$, $4v/\omega_p'$ and $8v/\omega_p'$. The left-hand panels show the values of the induced linear density at selected positions $\beta = \pi/4$, $\pi/8$ and $\pi/16$, as a function of time. The central panels show the whole variation of the induced linear density along the trajectory circle ($0 \leqslant \varphi < 2\pi$) for large enough times ($t/T_0 = 20, 10, 5$), such that in all cases the stationary state has been reached. The values indicated by vertical straight lines correspond to the saturation values (for the particular positions $\beta = \pi/4$, $\pi/8$ and $\pi/16$) shown in the left-hand panels. Finally, the panels on the right illustrate the whole behaviour of λ_{ind}. These wake structures rotate with the particle once the final equilibrium state is reached (i.e., they are stationary with respect to the moving particle). Notice in the last case the very asymmetric behaviour of λ_{ind} for points ahead of and behind the particle; this is due to the fact that for the large radius value ($a = 8v/\omega_p'$) chosen in this case the induced charge density has relaxed to equilibrium when the particle returns to a previously explored point (this is because the value of $T_0 = 2\pi a/v$ in this case is much larger than γ^{-1}). We also note that this particular result agrees very closely with the image of a 'linear' wake bent around a circle of radius a; this simple image applies when the wavelength of the wake, $2\pi v/\omega_p'$, is much smaller that $2\pi a$.

In figure 4 we show the value of the induced potential on points along the trajectory with $\beta = 0$ and $\pi/8$. In the first case we notice the steplike build-up of the asymptotic value through abrupt jumps every time a new circuit is completed. The case $\beta = 0$ gives the value of the induced potential applied to the charge itself. It shows a more rapid convergence to the saturation values after some initial fluctuations.

A picture of the complete angular variation of the induced potential after the asymptotic behaviour is obtained is shown in figure 5, for $t = 10T_0$. This may also be interpreted with the image of a wake potential wrapped around itself along a circle; but one should notice that the values are modified with respect to those for a particle in rectilinear motion due to the periodic matching conditions; i.e., in the present case, the oscillatory wake potential is simultaneously ahead of as well as behind the particle once the equilibrium state is achieved. A still more complete view of the spatial dependence of the rotating wake potential is shown in figure 6, where we show the induced potential on the plane $z = 0$, i.e. $\phi_{ind}(\rho, \varphi, z = 0)$, which illustrates more completely the whirling behaviour.

Finally, we have calculated the evolution of the instantaneous stopping power values, $S(t)/S_B$, using equations (18) and (19), and the results are shown in figure 7 for three values of the orbit radius: $a = 2v/\omega_p'$, $4v/\omega_p'$ and $8v/\omega_p'$. As may be observed, the approach to the asymptotic value, $S_A = \lim_{t\to\infty} S(t)$, is produced through a sequence of steps of decreasing height. In addition, the height of these steps also decreases when the value of a increases. The reason for this behaviour is again the effect of the damping constant γ. It may be shown that in the limit $\gamma \to 0$ the heights of all the steps become equal and the stopping power value increases without limit for the three cases shown. The controlling effect of γ may be illustrated in particular for the case of largest radius ($a = 8v/\omega_p'$) by comparing with figure 3 (bottom right panel), which shows that the wake is strongly attenuated in the time taken by the particle to complete a circuit ($T = 2\pi a/v \gg \gamma^{-1}$). This also explains the fast approach to equilibrium of the stopping value in this case; in particular, we notice that in the sudden initial rise of the stopping power the particle nearly attains the final saturation value.

The three cases shown here correspond to *positive phase matching* conditions. This occurs whenever the value of the orbit radius is of the form $a = \kappa v/\omega_p'$, where κ is an integer number. In these cases, there is an always positive addition of terms in the series of contributions to the induced charge and potential, equation (11), yielding a maximum accumulative effect and therefore a maximum stopping power. In other words, this corresponds to a *resonant* behaviour.

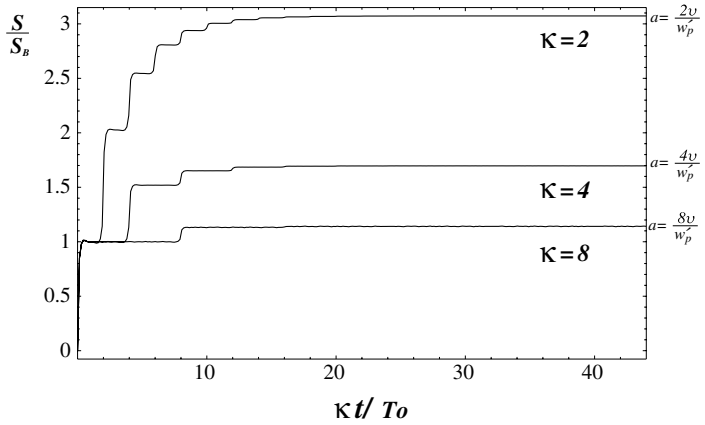

Figure 7. Stopping power, $S(t) = \mathrm{d}E/\mathrm{d}l$ (normalized to the stopping value for a straight trajectory, S_B), as a function of time, for $v = 2.7$ au, $\omega_p = 1.364 \times 10^{-3}$ au, $\gamma = 0.1\omega_p$ and for three values of the orbit radius: $a = 2v/\omega'_p$, $4v/\omega'_p$ and $8v/\omega'_p$.

For intermediate values of a the subsequent terms in the series (11) are affected by variable phases, leading to positive and negative contributions, and hence to smaller final stopping values.

In order to show the importance of these effects we compare the final stopping power values with that corresponding to a particle in straight line motion (to be called the Bohr stopping value) given by

$$S_B = \frac{(Ze\omega_p)^2}{v\omega'_p} \int_0^\infty \frac{\sin(\omega'_p\xi/v)}{(\rho_0^2+\xi^2)^{\frac{3}{2}}} \mathrm{e}^{-\gamma\xi/2v}\, \xi\, \mathrm{d}\xi, \tag{19}$$

which for small values of γ reduces to a well known expression [2],

$$S_B \tilde{=} \frac{(Ze\omega_p)^2}{v^2} \ln\left(\frac{k_{max}v}{\omega_p}\right), \tag{20}$$

with $k_{max} = 1/\rho_0$.

In figure 8 we show the behaviour of the stopping power ratio S_A/S_B (where S_A is the asymptotic, or stationary, stopping power for the circular trajectory) versus the parameter $\kappa \equiv a\omega'_p/v$ (which may correspond for instance to varying the orbit radius a). By comparison with figure 3 of [13] we conclude that we obtain the same resonant behaviour in the energy loss for the stationary conditions considered in that work. We also note that the value of the adimensional damping parameter γ/ω_p determines the maximum stopping-enhancement values obtained for $\kappa = 1, 2, 3, \ldots$. In addition, we observe that *antiresonance* conditions may also be obtained for intermediate values of κ ($\kappa = 1.5, 2.5, \ldots$), where the stopping power drops to nearly zero values if the damping is small. These near-cancellation effects are due to negative interferences in the self-interaction of the charge with its own induced field, an effect that may be also particularly important in the case of circular motion (i.e., due to the circular motion, the conditions for positive or negative interference effects will arise).

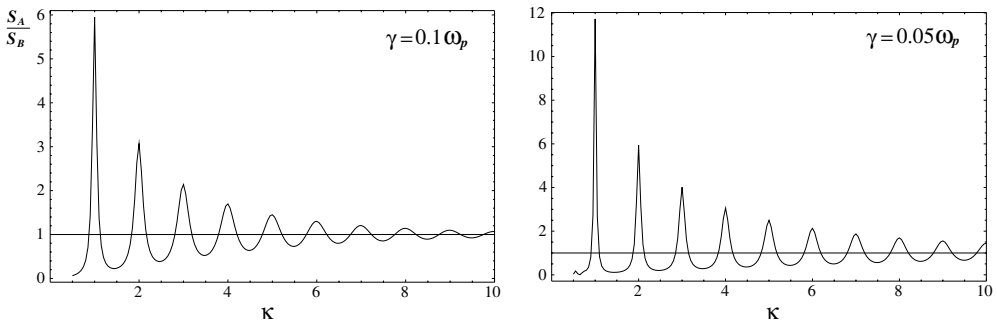

Figure 8. Stopping power ratio S_A/S_B (S_A being the asymptotic stationary value of the stopping power for a circular trajectory and S_B the stopping power for a particle with the same velocity but moving along a straight trajectory) versus the parameter $\kappa \equiv \omega_p'/v$, calculated for $v = 2.7$ au, $\omega_p = 1.364 \times 10^{-3}$ au, $\gamma = 0.1\omega_p$ and $0.05\omega_p$. A resonant behaviour is obtained, with maximum values for $\kappa = 1, 2, 3, \ldots$, and minimum values for $\kappa = 1.5, 2.5, 3.5, \ldots$ (antiresonance conditions). This resonant behaviour becomes more pronounced the smaller the value of the damping term γ/ω_p.

4. Conclusions

We have described the main characteristics of the induced charges and potential corresponding to charged particles moving in circular trajectories within a plasma.

The result for the induced potential shows the formation of a 'rotating wake' pattern, which may be explained by the image of a linear wake wrapped around itself in a circular way and subject to the necessary phase matching conditions.

The self-interaction of the particle is strongly affected by the periodical shape of the induced field. As a result, the energy loss rate shows a resonant effect which depends on the matching conditions, through the values of $a\omega_p'/v$ and of the adimensional damping parameter γ/ω_p, and may produce a significant enhancement of the energy loss with respect to the reference value corresponding to particles moving with the same speed but in a straight-line trajectory.

The inclusion of damping effects in the response function becomes essential in order to obtain a non-divergent stationary limit at large times due to an accumulation of effects.

The present results serve to understand the physical origin of the resonant effect in the energy loss of ions in circular trajectories within magnetized plasmas recently predicted by Nersisyan [13] for classical plasmas and derived also by Steinberg and Ortner [14] for dense quantum plasmas. These previous studies describe the asymptotic resonant behaviour which may be characterized by a stationary solution in the rotating frame. In addition to explaining this 'stationary' case, we analyse here in detail the previous transitory behaviour; this may be of interest to describe the time evolution of the local perturbations and fluctuations in the energy loss of ionized particles entering a region of high magnetic fields. Possible applications of these results to laboratory or astrophysical plasmas have been noted before [13, 14].

Acknowledgments

One of us (IVP) would like to acknowledge the Universidad of Valladolid for travel support, which made this collaboration possible. Financial support for this work was provided by FONCYT/ANPCYT of Argentina (project PICT 0303579) and the Spanish MCT (project BFM2000-1050-C02-01).

References

[1] Bohr A 1948 K. Dan. Vidensk. Selsk., *Mat.-Fys. Medd.* **24** no 19
[2] Pines D and Bohm D 1952 *Phys. Rev.* **85** 338
[3] Neufeld J and Ritchie R H 1955 *Phys. Rev.* **98** 1632
[4] Stenflo L, Yu M Y and Shukla P K 1973 *Phys. Fluids* **16** 450
[5] Vager Z and Gemmell D S 1976 *Phys. Rev. Lett.* **37** 1352
[6] Arista N R 1978 *Phys. Rev.* B **18** 1
[7] Echenique P M, Ritchie R H and Brandt W 1979 *Phys. Rev.* B **20** 2567
[8] Basbas G and Ritchie R H 1982 *Phys. Rev.* A **25** 1943
[9] Kononets Y V and Filippov G M 1982 *Sov. Phys.–JETP* **56** 547
Filippov G M 1992 *Sov. Phys.–JETP* **74** 871
[10] Gemmell D S and Vager Z 1985 *Treatise on Heavy-Ion Science* vol 6, ed D Allan Bromley (New York: Plenum) p 243
[11] D'Avanzo J D, Lontano M and Bortigon P F 1993 *Phys. Rev.* E **47** 3574
[12] Bringa E M and Arista N R 1996 *Phys. Rev.* E **54** 4101
[13] Nersisyan H B 1998 *Phys. Rev.* E **58** 3686
[14] Steinberg M and Ortner J 2001 *Phys. Rev.* E **63** 046401